small
NANO MICRO

Patterned Polymer Carpets

Ihsan Amin, Marin Steenackers, Ning Zhang, René Schubel, André Beyer, Armin Gölzhäuser, and Rainer Jordan**

***F**or the development of polymer carpets as active devices for micro- and nanotechnology, a control of the polymer carpet morphology and especially control of the stimulus responsive polymer brush is needed. Here, we report on the first example for the fabrication of patterned polymer carpets. On a two-dimensional framework of fully crosslinked and chemically patterned nanosheets, polymer brushes of styrene and 4-vinyl pyridine were grafted by self-initiated surface photopolymerization and photografting (SIPGP). It was found that polymer grafting by SIPGP occurred over the entire nanosheets but with a preferred grafting on the amino functionalized nanosheet areas. This results in continuous polymer carpets with an intact nanosheet framework but with amplification of the chemical patterning into a three dimensional topography of the grafted polymer brush. In the case of negative patterned nanosheets, the patterned carpet could be prepared as freestanding ultrathin membranes. Furthermore, swelling experiments with poly(4-vinyl pyridine) carpets showed that the patterns induces a directional buckling of the flexible polymer carpet. This may open the possibility of the development of micro- or nanoactuator devices with anisotropic responds upon environmental changes.*

1. Introduction

Recently, we introduced a new class of polymer material: so-called "polymer carpets"—a freestanding or supported crosslinked self-assembled monolayer (SAM) on which a polymer brush was grown by surface-initiated polymerization.[1] Polymer carpets can be created with lateral dimensions of centimeters and thicknesses from some to several hundreds of nanometers, depending on the surface-initiated polymerization time. Similar to substrate-bonded polymer brushes, polymer carpets react spontaneously to environmental changes by swelling or collapse of the polymer layer, causing changes to, e.g., the optical properties and wettability.[2–4] However, since the flexible polymer carpet is not covalently linked to a solid substrate, it reacts instantaneously by an additional and quite significant change of its overall morphology; namely, by a buckling of the entire carpet layer. Such buckling is characteristic for thin, soft-matter films such as crosslinked (elastomeric) polymers or polyelectrolyte multilayers,[5,6] or elastomers modified with rigid thin films.[7–10] The buckling, along with the polymer layer collapse, may be used for the development of new actuating and sensing devices, taking advantage of the ultrathin but macroscopically large and robust polymer carpet of minimal mass. Huck and coworkers[11,12] presented a similar system of (crosslinked) polymer brushes attached to ultrathin gold films. Although a 'substrate' is still present in the form of a thin gold layer, the polymer brush films are otherwise free-standing. For the development of free-standing polymer brushes on ultrathin metal layers[12] or, as in this case, polymer carpets

Dr. I. Amin, R. Schubel, Prof. R. Jordan
Department Chemie
Technische Universität Dresden
Zellescher Weg 19, 01069 Dresden, Germany
E-mail: Rainer.Jordan@tu-dresden.de
Dr. M. Steenackers
Institute for Advanced Study
Technische Universität München
Arcisstr. 21, 80333 München, Germany
Dr. M. Steenackers, Dr. N. Zhang, Prof. R. Jordan
Wacker-Lehrstuhl für Makromolekulare Chemie
Technische Universität München
Lichtenbergstrasse 4, 85747 Garching, Germany
Dr. I. Amin, Dr. A. Beyer, Prof. A. Gölzhäuser
Physik Supramolekularer Systeme
Universität Bielefeld
Universitätsstraße 25, 33615 Bielefeld, Germany
E-mail: goelzhaeuser@uni-bielefeld.de

DOI: 10.1002/smll.201001658

as active devices for micro- and nanotechnology, control of the polymer carpet morphology and especially control of the stimulus-responsive polymer brush is needed. There are several straight-forward possibilities to tailor the overall shape of the polymer carpet on various length scales, such as simple mechanical cutting or destructive lithographic techniques using, for example, ion beams, rolling, bending, folding, etc.[13] Here, we report on an approach to control the polymer brush layer morphology while preserving a continuous nanosheet of crosslinked SAM; in other words, keeping the 2D framework of the nanosheet intact and only introducing a chemically patterned template for selective or preferential polymer grafting. Such systems were recently proposed in an excellent review by Schlüter et al.[14]

2. Results and Discussion

For the preparation of patterned polymer carpets, a chemically patterned nanosheet was first prepared. As recently reported, electron lithography was used along with an exchange reaction to create fully crosslinked and chemically patterned SAMs with areas of biphenyl thiol (cBT) and 4'-amino-1,1'-biphenyl-4-thiol (cABT) on gold.[15] This 2D template was then used for surface-initiated photopolymerization. The complete preparation of patterned polymer carpets is outlined in **Scheme 1**.

The positive- or negative-patterned cBT/cABT nanosheets were detached from the gold substrate and transferred to a silicon nitride substrate as a support. The substrates were then immersed in bulk styrene and irradiated with UV light (spectral range: 300–400 nm, λ_{max} = 350 nm) for 30 min to form a polystyrene layer by self-initiated surface photopolymerization and photografting (SIPGP), analogous to the fabrication of homogeneous polymer carpets.[1]

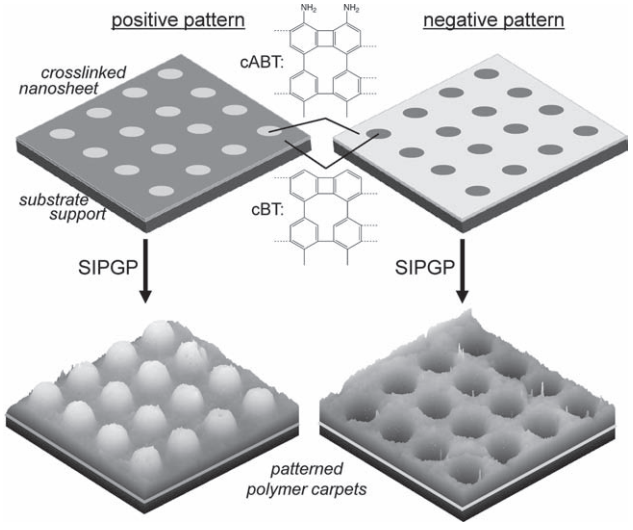

Scheme 1. Fabrication of patterned polymer carpets. Positive- or negative-patterned and fully crosslinked nanosheets on a silicon support were used for the grafting of vinyl monomers via self-initiated surface photopolymerization and photografting (SIPGP). Grafting occurred on the entire nanosheet, however, preferred grafting was observed on the cABT areas, resulting in a direct amplification of the chemical pattern of the nanosheets. The images of the patterned polymer carpets (below) are 3D representations of the AFM scans shown in Figure 2.

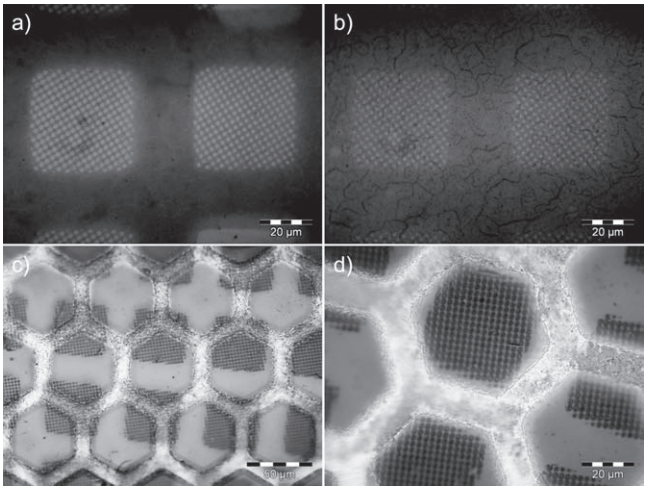

Figure 1. Optical micrographs of supported and freestanding patterned polymer carpets. a) Optical micrograph of positive-patterned and b) negative-patterned polystyrene carpets supported by a silicon nitride substrate. c,d) Freestanding negative-patterned polystyrene carpets on a TEM copper grid at different magnifications.

Figure 1 shows the optical micrographs of a) positive- and b) negative-patterned nanosheets after the SIPGP with styrene. For both cases, the formation of amplified patterns is clearly visible. The patterned povlymer carpets were then detached from the substrate and transferred to TEM grids following the same protocol as reported previously.[1] In the micrographs (Figure 1c,d) the successful preparation of freestanding patterned polymer carpets is shown. For negative-patterned carpets, the ultrathin membranes could be directly transferred as intact sheets with only minor defects. However, in the case of positive patterning, preferred defects and detachment around the patterned areas were noticed during the transfer process (see Supporting Information (SI), Figure S1). This is probably because of the very thin polymer layer created on the large cBT areas.

The SIPGP grafting mechanism relies on the radical abstraction of surface-bonded groups by the photoactivated vinyl monomers.[16–22] The probability of the radical abstraction reaction which leads to polymer grafting by free-radical, surface-initiated polymerization is determined by the bond dissociation energy (BDE) of the respective surface groups. A low BDE results in facilitated abstraction and thus increased polymer grafting, higher grafting density, and, because of the brush scaling law,[23–25] a thicker polymer layer. Additionally, during the ongoing SIPGP grafting reaction, radical abstraction will occur on already grafted polymer chains, leading to branching. However, in a previous study for the SIPGP of vinyl monomers on crosslinked SAMs of biphenyl thiols with different end-functions for the formation of polymer brushes, it was found that the branching is significantly higher than expected for free-radical, surface-initiated polymerization.[26] In the same study, we investigated different grafting efficiencies as a function of the BDE of surface-bonded functions using crosslinked and differently functionalized biphenyl SAMs, specifically on cABT and cBT surfaces. The BDE of

NANO MICRO small

the aromatic C–H bond for cBT is about 111 kcal mol^{-1} and for the N–H bond for cABT only 89.3 kcal mol^{-1}. Because for both surface groups the BDE is relatively low, grafting was observed on both surfaces but with a significantly thicker polystyrene brush formation on cABT areas. **Figure 2** shows the AFM scans of a single-structure array, along with detailed scans and their section analysis of supported positive- and negative-patterned cBT/cABT nanosheets after the SIPGP of styrene and a thorough cleaning procedure.

As expected, polymer grafting occurred over the entirety of the nanosheets, but with significantly thicker polystyrene (PS) brushes formed on the cABT areas. In both cases, for negative and positive patterns, the height difference within the formed PS layer is almost the same and calculates to 10–12 nm. The period (center-to-center spacing) of the dots is 2.45 μm and of wells 2.56 μm; thus, this is a direct transfer

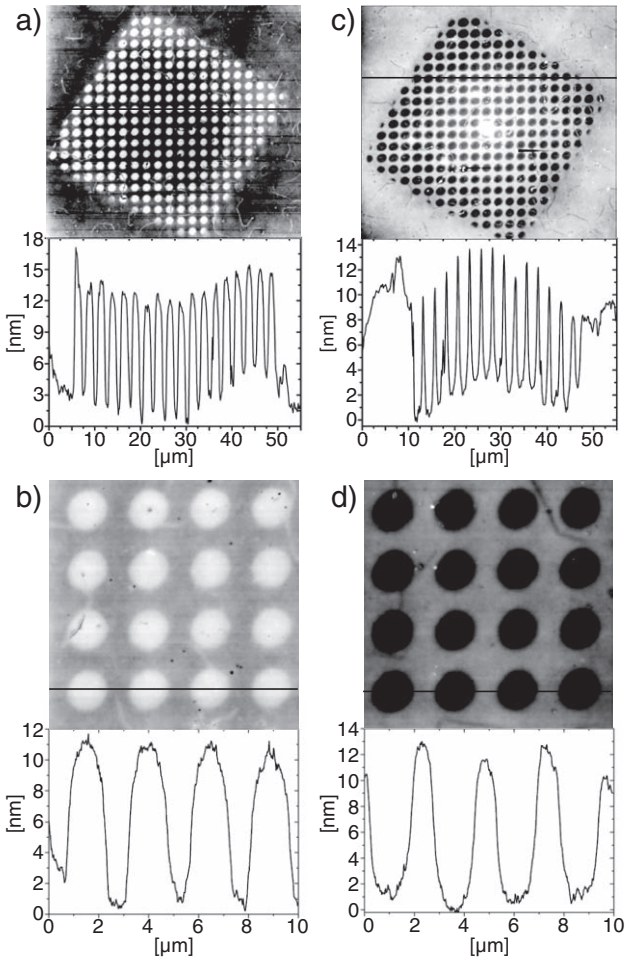

Figure 2. AFM scans of a,b) positive- and c,d) negative-patterned polystyrene carpets on a silicon nitride substrate support. a) Overview scan (above) and section analysis (below) of a row of PS dots created by the preferred grafting of styrene on the cABT areas (the apparent curvature of the scan is due to plane fitting). b) A detailed AFM scan reveals a height difference of approximately 10–12 nm. c) Overview scan (above) and section analysis (below) of a row of wells created from negative cBT/cABT patterned nanosheets. d) Detailed scan of the same structure. Section analysis of an arbitrary row of wells gives a depth of 11–12 nm.

of the structure period of the R1.2/1.3 carbon foil mask of 2.5 μm. The average full-width-at-half-maxima of wells and dots are 1.54 and 1.49 μm and thus somewhat larger than the mask openings of 1.2 μm, partially due to the lateral relaxation of the polymer brush film grown on the nanosheet framework,[27–32] but mainly because of the experimental setup, which causes a small gap to exist between the mask and the substrate plane. AFM analysis of the unpatterned areas of cBT or cABT reveal a smooth and uniform PS brush without any distinct surface topography (Figure 2a,c). This is in agreement with our pervious observations, as buckling of supported PS carpets is not observable for PS brush layer thicknesses below approximately 70 nm.[1] To determine the absolute layer thicknesses for the PS brush formed on cABT and cBT surfaces, additional AFM investigations were performed at the edges of the carpets (see SI, Figure S2). At the cBT edges (negative patterning) the PS layer thickness is calculated as approximately 17 ± 2 nm, and at the cABT edges (positive patterning) as 24 ± 2 nm. Thus, the thickness of the polymer layer formed on the cABT and cBT functionalized surface areas is almost identical and the relative difference of the layer thicknesses formed on both surfaces is nearly the same.

Besides styrene, SIPGP was also performed with 4-vinyl pyridine (4VP) on negatively patterned cBT/cABT nanosheets. Nanosheet preparation and transfer onto a silicon nitride support was carried out as described above, only this time a R1/4 carbon foil mask (hole diameter: 2 μm, center-to-center distance: 4 μm) was used. The SIPGP was performed for 4 h and the cleaning procedure was carried out with a different set of solvents to ensure quantitative removal of nongrafted polymer.[1]

Figure 3a,b shows AFM scans of the obtained patterned areas. As for styrene, the SIPGP with 4VP amplifies the chemical pattern of the nanosheet into a 3D-patterned polymer carpet. Again, grafting occurs on the entire fully crosslinked nanosheet, but with preferred grafting on the cABT areas due to the lower BDE of the N–H bond of the 4'-amino group. Since the polymerization time was four times longer, the resulting P4VP layer is significantly thicker and the height difference between the P4VP brushes formed on cBT and cABT regions is significant, approximately 120 nm higher (see SI, Figure S3). In contrast to the thin PS carpet where no buckling was observed, the thicker P4VP carpet shows buckling in the collapsed (dry) state. The topography of unpatterned cABT areas (Figure 3c) is very similar to our previous observations on thick homogeneous P4VP carpets under bad solvent conditions (dry collapsed state).[1] Analogous to our previous experiments on the stimulus-responsive P4VP carpets, the patterned P4VP carpet was submerged in ethanol (good solvent) and the dry, opaque carpet instantaneously became optically transparent, as reported before. Interestingly, AFM analysis on the partially swollen P4VP carpet gave a different overall morphology, as displayed in Figure 3d–f). The carpet morphology of unpatterned areas was changed significantly, and, most interestingly, within the pattered areas the buckling direction of the swollen carpet correlated in a characteristic way to the cBT/cABT patterning, forming directed buckles that originated and ended between adjacent cBT wells (Figure 3e). Apparently, the changed

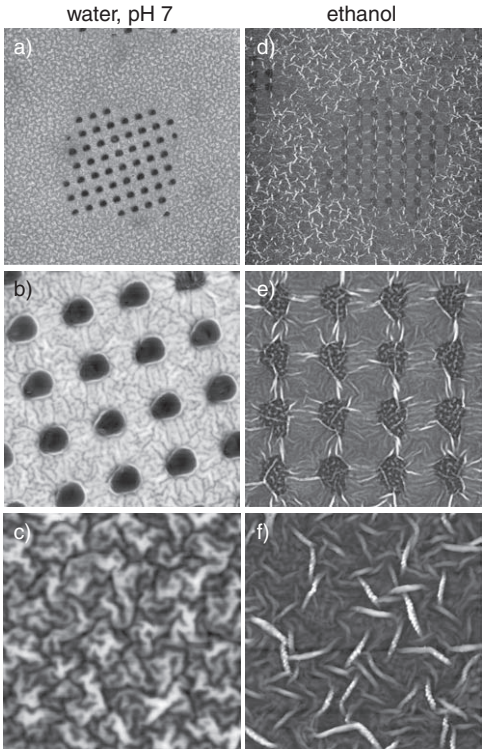

Figure 3. AFM scans of a patterned P4VP carpet. a) Overview scan (80 μm × 80 μm; z: 213 nm) of the negative cBT/cABT patterned area as prepared. b) Detailed 20 μm × 20 μm; z: 166 nm scan of same structure as in (a). c) Detailed scan of unpatterned P4VP carpet grown on a homogeneous cABT area (10 μm × 10 μm; z: 370 nm). d) Overview scan (80 μm × 80 μm; z: 400 nm) at ambient conditions of the same area as in (a) after 15 min exposure to ethanol. e) Detailed scan (20 μm × 20 μm; z: 120 nm) of same structure. The correlation of the patterning and polymer carpet folding is clearly visible. f) Detailed scan of unpatterned P4VP carpet grown on a homogeneous cABT area after ethanol treatment with a significantly changed surface topography but no oriented buckling (10 μm × 10 μm; z: 370 nm).

overall structure along with the additional patterning has a directive effect upon the orientation of the buckling. The described morphology change was found to be fully reversible (see SI, Figure S4). Treatment with water (bad solvent) resulted in morphology very similar to the one depicted in Figure 3a–c, but treatment with ethanol gave again the directional buckling as shown in Figure 3d–f.

Ordered buckling as a function of surface patterning has been observed before on soft elastomeric polymer substrates modified with a rigid film, such as evaporated metals,[10,,7] or silica.[8,10] As outlined by Whitesides et al.[8,10] ordered/directional buckling is caused by the anisotropic release of compressive stress and can be controlled by, for example, the shape[7,10] as well as the size[9] of the patterns relative to the buckling wavelength, λ. Comparison of Figure 3b and e shows clearly that for the same sample and on the same spot no directional buckling (after water treatment, Figure 3b) or strong directional buckling (after ethanol treatment, Figure 3e) of the thin polymer carpet is observable. Analyzing the buckling wavelength at isotropic areas for both states gave a λ of 1.24 ± 0.14 μm after water treatment but $\lambda = 368 \pm 34$ nm after treatment with ethanol. As the pattern size (well diameter) is about 2.5 μm and thus in the same dimension of λ after water treatment, no significant directional buckling is observable in this state. However, after ethanol treatment, λ is much smaller than the pattern dimension and significant directional buckling characterizes the morphology of the patterned areas of the polymer carpet. Our observation is in nice agreement with the findings reported by Hendricks and Lee for a quite different PDMS/silica system that displayed a strikingly similar surface topography.[9] As the ordered buckling of the polymer carpet may allow the creation of responsive polymer carpets as sensor or actuator devices with unidirectional or at least anisotropic properties, we are currently investigating this relationship in greater detail.

3. Conclusion

In summary, we have shown that patterned polymer carpets can be prepared from chemically patterned, fully crosslinked nanosheets of biphenyl thiols by amplification, using self-initiated photopolymerization and photografting of vinyl monomers. Both, positive- and negative-patterned polymer carpets can be fabricated. Swelling of the patterned polymer brush layer in good solvents results in a reversible and distinct morphology change of the flexible polymer carpet. The observed increased buckling of the partially swollen carpets is reversible and, moreover, correlates directly to the patterning. In agreement with previous studies on buckling systems, directional buckling is observable if the buckling wavelength is much smaller than the pattern dimensions. The directional buckling may be useful for the development of sensors and actuators with anisotropic responds.[33] Related experiments are currently underway in our laboratories.

4. Experimental Section

Patterned Nanosheets: Fully crosslinked, patterned nanosheets were prepared by employing the procedures described before.[15] In short, a flat Au substrate was first immersed in a 10 mM solution of 4'-nitro-1,1′-biphenyl-4-thiol (NBT, purchased from Taros Chemicals) or 1,1′-biphenyl-4-thiol (BPT, purchased from Platte Valley Scientific) in *N*,*N*-dimethylformamide (DMF p.a., purchased from VWR, dried with 0.4 nm molecular sieve) for 3 days at room temperature. The sample was rinsed with DMF and ethanol and dried in a stream of nitrogen. Patterning/partially crosslinking of the NBT or BT SAM was performed in high vacuum ($<5*10^{-7}$ mbar, where 1 bar = 10^5 Pa) with an electron floodgun (Specs FG20) at an electron energy of 100 eV and dose of 20 mC cm^{-2}. A carbon foil mask (R1.2/1.3 or R1/4, Quantifoil Micro Tools, Jena, Germany) was used as a stencil mask. The patterned/partially crosslinked NBT or BT SAMs were then immersed in a 10 mM solution of BPT or NBT, respectively, in dry DMF at 55 °C for 1 h to 3 days. The sample was rinsed in DMF and ethanol and finally dried in a nitrogen stream. The whole sample was again exposed to 100 eV electrons with a dose of 40 mC cm^{-2}, resulting in a fully crosslinked positive- or negative-patterned SAM. Crosslinked nanosheets were prepared by detaching the SAM from the gold substrate and transferring it onto a silicon support with a 150 nm thick silicon nitride layer, following the previously published procedure.[15]

NANO MICRO small

Self-Initiated Photografting and Photopolymerization (SIPGP): SIPGP was performed as reported previously.[16,20,22,26,29,34,35] In brief, the fully crosslinked patterned nanosheets on silicon support were immersed into approx. 1 mL of freshly distilled and degassed styrene, or 4-vinyl pyridine (4VP) (Fluka) in a Duran glass photoreaction vial. Polymerization was performed under irradiation with UV-light (300–400 nm spectral distribution, $\lambda_{max} = 350$ nm) under an argon atmosphere at room temperature for 30 min (for styrene) and 4 h (for 4-vinyl pyridine). After the polymerization, the samples were removed from the reaction solution and immediately washed with good solvents for the particular polymer (toluene for polystyrene and ethanol for poly(4-vinyl pyridine). The samples were additionally cleaned in ethyl acetate and ethanol.

Freestanding Patterned Carpets: The patterned Carpets were obtained by dissolving the silicon nitride layer in hydrofluoric acid (48%) and transferring the free patterned carpets onto Cu TEM grids (400 mesh, Plano, Wetzlar, Germany).

Microscopy: Optical microscopy images were taken with an Olympus BX51 (Olympus, Hamburg, Germany). Atomic force microscopy scans were performed with an NTEGRA atomic force microscope from NT-MDT (Eindhoven, The Netherlands). All scans were performed in noncontact mode using standard tips and under ambient conditions.

Determination of Buckling Wavelength: Buckling wavelengths were determined from AFM scans depicted in Figure 3. Arbitrarily choosen line profiles of polymer carpet areas with isotropic buckling were analyzed and peak-to-peak values (n = 6) averaged. For P4VP carpets, after water treatment the buckling wavelength of 1.24 ± 0.14 μm and after ethanol treatment of 368 ± 34 nm was found.

Supporting Information

Supporting Information is available from the Wiley Online Library or from the author.

Acknowledgements

This work was partially supported by the International Graduate School for Science and Engineering (IGSSE) at the Technische Universität München. M.S. acknowledges support from the Institute for Advanced Study (IAS) of the Technische Universität München.

[1] I. Amin, M. Steenackers, N. Zhang, A. Beyer, X. Zhang, T. Pirzer, T. Hugel, R. Jordan, A. Gölzhäuser, *Small* **2010**, *6*, 1623–1630.
[2] F. Zhou, W. T. S. Huck, *Phys. Chem. Chem. Phys.* **2006**, *8*, 3815–3823.
[3] R. Toomey, M. Tirrell, *Annu. Rev. Phys. Chem.* **2008**, *59*, 493–517.
[4] A. Kumar, A. Srivastava, I. Y. Galaev, B. Mattiasson, *Prog. Polym. Sci.* **2007**, *32*, 1205–1237.
[5] J. Y. Chung, A. J. Nolte, C. M. Stafford, *Adv. Mater.* **2010**, in press, (DOI: 10.1002/adma.201001759).
[6] C. M. Stafford, C. Harrison, K. L. Beers, A. Karim, E. J. Amis, M. R. VanLandingham, H. C. Kim, W. Volksen, R. D. Miller, E. E. Simonyi, *Nat Mater* **2004**, *3*, 545–550.
[7] W. T. S. Huck, N. Bowden, P. Onck, T. Pardoen, J. W. Hutchinson, G. M. Whitesides, *Langmuir* **2000**, *16*, 3497–3501.
[8] N. Bowden, W. T. S. Huck, K. E. Paul, G. M. Whitesides, *Appl. Phys. Lett.* **1999**, *75*, 2557–2559.
[9] T. R. Hendricks, I. Lee, *Nano Lett.* **2007**, *7*, 372–379.
[10] N. Bowden, S. Brittain, A. G. Evans, J. W. Hutchinson, G. M. Whitesides, *Nature* **1998**, *393*, 146–149.
[11] M. Wang, J. E. Comrie, Y. Bai, X. He, S. Guo, W. T. S. Huck, *Adv. Funct. Mater.* **2009**, *19*, 2236–2243.
[12] T. S. Kelby, W. T. S. Huck, *Macromolecules* **2010**, *43*, 5382–5386.
[13] S. Singamaneni, M. E. McConney, V. V. Tsukruk, *ACS Nano* **2010**, *4*, 2327–2337.
[14] J. Sakamoto, J. van Heist, O. Lukin, A. D. Schlüter, *Angew. Chem. Int. Ed.* **2009**, *48*, 1030–1069.
[15] A. Beyer, A. Godt, I. Amin, C. T. Nottbohm, C. Schmidt, J. Zhao, A. Gölzhäuser, *Phys. Chem. Chem. Phys.* **2008**, *10*, 7233–7238.
[16] M. Steenackers, S. Q. Lud, M. Niedermeier, P. Bruno, D. M. Gruen, P. Feulner, M. Stutzmann, J. A. Garrido, R. Jordan, *J. Am. Chem. Soc.* **2007**, *129*, 15655–15661.
[17] H. Wang, H. R. Brown, *Macromol. Rapid Commun.* **2004**, *25*, 1095–1099.
[18] J. Deng, W. Yang, B. Ranby, *Macromol. Rapid Commun.* **2001**, *22*, 535–538.
[19] S. J. Li, C. G. Li, T. Li, J. J. Cheng, *Polymer Photochemistry Principles and Applications*, Fudan University Press, Shanghai **1993**, p.110.
[20] N. A. Hutter, A. Reitinger, N. Zhang, M. Steenackers, O. A. Williams, J. A. Garrido, R. Jordan, *Phys. Chem. Chem. Phys.* **2010**, *12*, 4360–4366.
[21] L. Faxälv, T. Ekblad, B. Liedberg, T. L. Lindahl, *Acta Biomater.* **2010**, *6*, 2599–2608.
[22] M. Steenackers, I. Sharp, K. Larson, N. Hutter, M. Stutzmann, R. Jordan, *Chem. Mater.* **2010**, *22*, 272–278.
[23] S. Alexander, *J. Phys. (Paris)* **1977**, *38*, 977–981.
[24] S. T. Milner, *Science* **1991**, *251*, 905–914.
[25] P. G. de Gennes, *Adv. Colloid Interface Sci.* **1987**, *27*, 189–209.
[26] M. Steenackers, A. Küller, S. Stoycheva, M. Grunze, R. Jordan, *Langmuir* **2009**, *25*, 2225–2231.
[27] U. Schmelmer, A. Paul, A. Küller, M. Steenackers, A. Ulman, M. Grunze, A. Gölzhäuser, R. Jordan, *Small* **2007**, *3*, 459–465.
[28] M. Steenackers, A. Küller, N. Ballav, M. Zharnikov, M. Grunze, R. Jordan, *Small* **2007**, *3*, 1764–1773.
[29] M. Steenackers, R. Jordan, A. Küller, M. Grunze, *Adv. Mater.* **2009**, *21*, 2921–2925.
[30] M. Patra, P. Linse, *Nano Lett.* **2006**, *6*, 133–137.
[31] B. Lee, C. Lo, S. Seifert, N. L. D. Rago, R. E. Winans, P. Thiyagarajan, *Macromolecules* **2007**, *40*, 4235–4243.
[32] M. Kaholek, W. Lee, B. LaMattina, K. C. Caster, S. Zauscher, *Nano Lett.* **2004**, *4*, 373–376.
[33] During production of this publication, a themed issue on the "Physics of buckling" was published: *Soft Matter* **2010**, *6*, (22), 5647–5818.
[34] S. Gupta, M. Agrawal, M. Conrad, N. Hutter, P. Olk, F. Simon, L. M. Eng, M. Stamm, R. Jordan, *Adv. Funct. Mater.* **2010**, *20*, 1756–1761.
[35] N. Zhang, M. Steenackers, R. Luxenhofer, R. Jordan, *Macromolecules* **2009**, *42*, 5345–5351.

Received: September 20, 2010
Revised: November 5, 2010
Published online: December 29, 2010

